Synthesis, Characterization, anti- microbial, anti-cancer activity and docking studies of novel bioactive Schiff base ligand derived from sulphaclozine with some Metal(II) chelates and its Nanocomplexes

Tarek M.A. Ismail*[1], Abdel Razak M Tawfik[2], Doaa F.Sallam[3] and Samy M. Abu-El-Wafa[4]

[1,2,3,4] *Department of chemistry, Faculty of Education, Ain Shams University, Roxy, Cairo, Egypt.*
Corresponding Author: Tarek M.A Ismail

Abstract: *Both of novel Schiff base ligand, N-(6-chloropyrazin-2-yl)-4-{[(E)-(2 hydroxyphenyl)methylidene] amino}benzene- sulfonamide(CPHPMABS) derived from sulfaclozine and salicylaldehyde with its Co(II), Ni(II), Cu(II), Zn(II) and Cd(II) complexes have been synthesized and characterized using different instrumental analyses and spectroscopic methods to throw more light about their geometries. 3D modeling of the ligand and its Cd(II) complex can be used by DMOL3 program in Materials Studio program.The quantum-mechanical properties like molecular orbitals and molecular energies can be computed and the cluster calculations were performed. Also, Cu nanocomplexes III, VI, VII and VIII were synthesized in different media (EtOH, Cetyltrimethylammoniumbromide (CTAB), SpinaciaOleracea (SO) and MalvaParviflora (MP) respectively then characterized by Electronic spectra, Transmission electron microscope (TEM) images and XRD pattern. The electrical conductivity studies of some Cu nanocomplexes revealed that semiconductor behavior for these nano compounds.The Cu nanocomplexes were screened as an antitumor agent towards Hepatocellular carcinoma cell line (HepG-2) and compared with cis-platin. The antitumor data revealed that the Cu nanocomplexVI have antitumor activity nearly to the activity of cis-platin. The Schiff base ligand and its Cu nanocomplex III were tested as carbonic anhydrase (CAII) inhibitor. Molecular docking in the CA II active site attributed the promising inhibitory activity of Cu nanocomplexis more active than Schiff base ligand to the interaction of their sulfonamide moiety with the active site Zn^{2+} ion. These results indicated that sulfaclozine compounds promising as antitumor drugs. Schiff base ligand, its metal chelates and its Cu nanocomplexes were tested against antibacterial and antifungal. The Cu nanocomplex VI showed the highest activity.*

Key Words*: sulphaclozine compounds, Schiff bas, metal II complexes,Cu nanocomplexes,antimicrobial and antitumor activities, Molecular docking, 3D modeling, Electrical Conductivity Studies*

I. Introduction

Sulpha drugs can be used systematically as preventive and therapeutic agents against various diseases [1, 2].Theywere reported to be active against different type of bacteria and viruses [3] and have been used as drugs for diseases such as cancer [4] and tubercular [5]. The Schiff base complexes derived from sulfa drugs have gained good complexion ability and biological activities [6-9].Cu nanoparticles exhibit manyuses anddifferent applications in industry and medical field; they act as semiconductor, an anti-biotic, anti-bacterial, and anti-fungal agent [10, 11].We did not found any thing about the Schiff base ligand under investigation, metal(II) complexes and its nanocoordinationcomplex inliterature,so this work aimed to synthesizenovel Schiff base ligand derived from sulfaclosine and salysaldehyde. Alsotheir metal chelates and nanocomplexes were prepared. The prepared metal chelates are characterized byElemental and thermal analyses, molar conductance, IR, Mass, ^{1}HNMR, Electronic, ESR spectra and magnetic studies.Also,nanocomplexescharacterized by Electronic spectra, (TEM) images and XRD pattern.

The electrical conductivity on the solid state for Cu nanocomplexes I and II were measured.The docking study indicated that Cu nanocomplex is possibility inhibitors of cancer causing receptors which revealed that developing these sulphaclozine compounds as antitumor drugs.The synthesized ligand, its metal (II) chelates and its Cu nanocomplex for antimicrobial and antitumor activities were tested.

II. Experimental

2.1. Materials
All chemicals were obtained from Merck products, Aldrich and BDH. The solvents were methanol, ethanol, DMF and diethylether. These solvents were purified by the recommended methods [12].

2.2. Physical measurements
Physical measurements and the apparatus which used in this studywere present as in our publications [2, 13, and 14].

2.3. Synthesisof the Schiff base ligand
Synthesis of the Schiff base ligand was carried out by addition 2-hydroxy benzaldehyde(0.87 ml, 0.008 mol) to 50 ml of ethanolic solution of sulphaclosine (2.5 gm, 0.009 mol) and was refluxed for 8 hours,orange precipitate were formed, filtered off and recrystallized using ethanol. yeild 80%, m.p. 245°C for perepared ligand namely N-(6-chloropyrazin-2-yl)-4-{[(E)-(2 hydroxyphenyl)methylidene]amino}-benzenesulfonamide (CPHPMABS). Synthesis of the Schiff base ligand was showed schematically in Scheme 1.
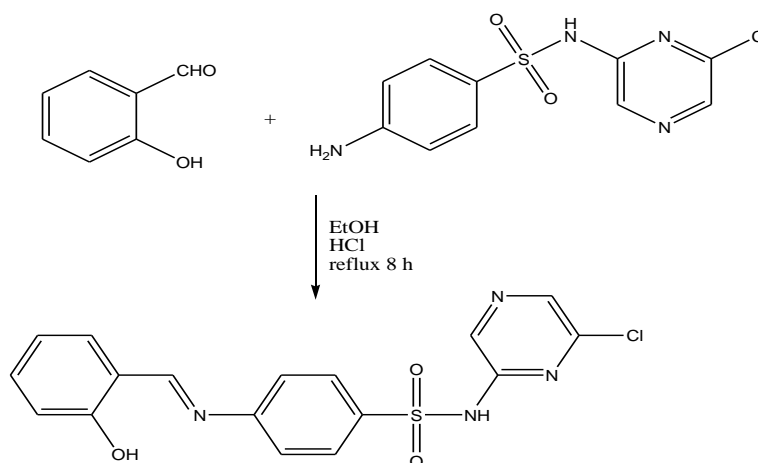
Scheme 1. Illustrated the synthesis of Schiff base ligand

-Elemental analysis of CPHPMABS: (Calcd %) C, 52.5;H,3.34;N, 14.4; S, 8.2
                                    (Found %) C, 52.08; H, 3.86;N, 13.87; S, 7.84

-UV-Vis spectra; λmax (nm), π- π* transition of the aromatic system exhibits band located at (278), the band within the (314) assigned to π- π* transition of the C=N groups. The band within the (392) is due to an intermolecular charge transfer within the whole molecule (CT).

-Mass spectrum of CPHPMABS ligand is shown in Fig.1.
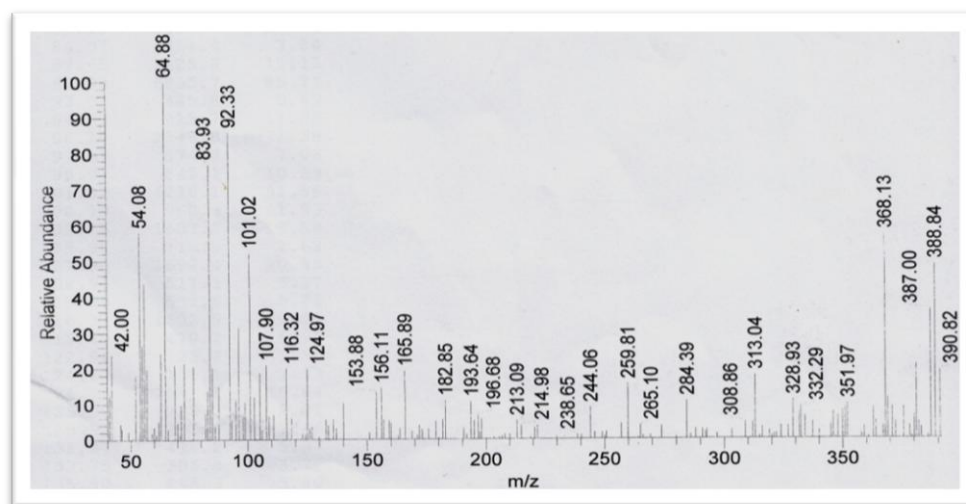
Fig. 1. Mass spectra of Schiff base ligand CPHPMABS

The Schiff base ligand CPHPMABS under investigation exhibits the molecular ion peak (m/e) = 388.5 as the same with the molecular weight of the ligand, also the isotope of the ligand has a peak with m/e value of M+2.Scheme 2represents the mechanism fragmentation of mass spectra of the ligand (CPHPMABS).
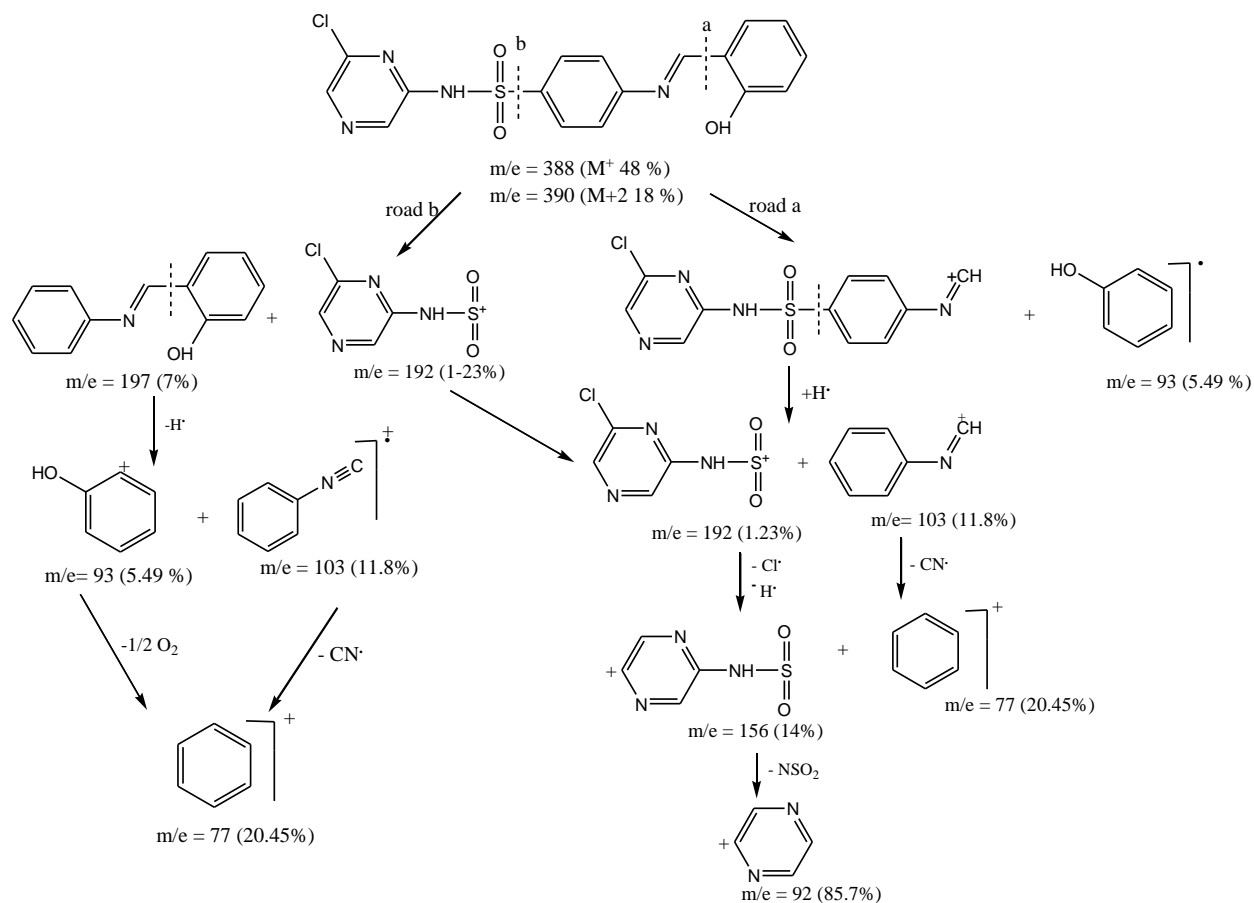
Scheme 2. Mechanism of mass fragmentation of Schiff base ligand

2.4. A.Synthesis of metal complexes

Ethanolic solution of metal nitrates of Co(II), Ni(II), Cu(II), Zn(II) or Cd(II) were added slowly to the ethanolic solution of the prepared ligand in a 2:1 (L:M) molar ratio and was refluxed in a hot plate for 6 -8 hours.

The solid complexes filtered off after cooling to room temperature, washed with small amounts of hot ethanol, bidistilled water, diethylether and dried in vaccum desiccator over anhydrous $CaCl_2$.

2.4. B. synthesis of Cu Nanocomplex

Cu nanocomplexesIII, VI, VII and VIII weresynthesized in different media (EtOH, Cetyltrimethylammoniumbromide (CTAB), SpinaciaOleracea (SO) and MalvaParviflora (MP) respectively according to in our publications [2, 13,14] and previously mentioned elsewhere[15,16, 17]. The nanostructure was characterized by X-ray diffraction (XRD), Transmission electron microscope (TEM) and electronic spectra studies.TEM picture of all prepared Cu nanocomplexes showed a small particle size in nano scale range with a nano feature products, Figs.2 and 3. The particles size values of nanocomplexesIII, VI, VII and VIII are14nm,8.5 nm,13.5 nm and 18.7 nm respectively.
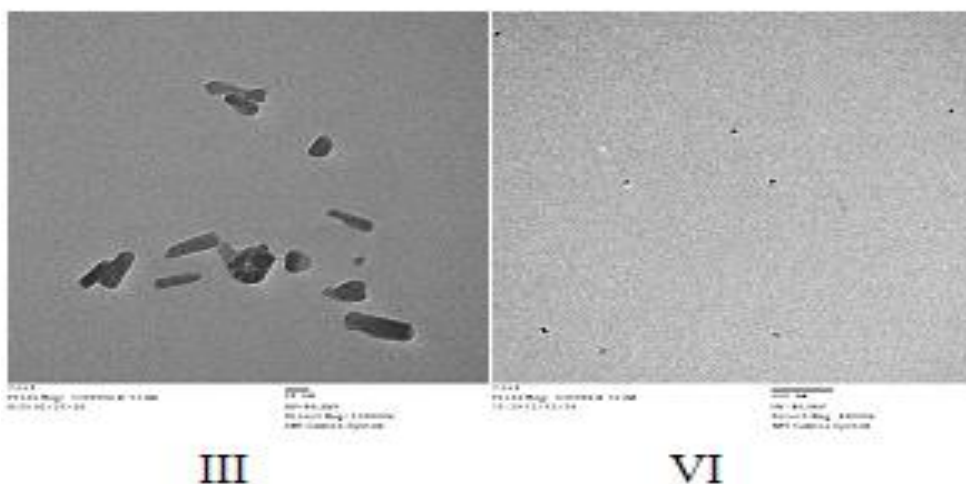
Fig.2. TEM images of Cu nanocomplexes IIIand VI
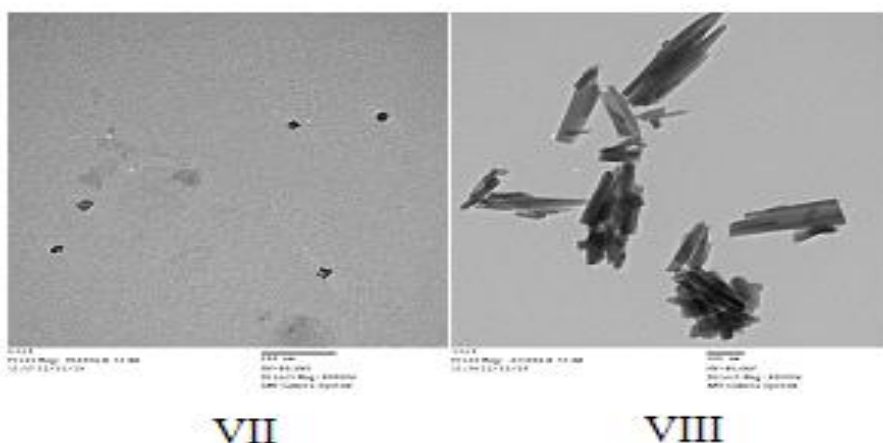
Fig. 3. TEM images of Cu nanocomplexesVII and VIII

X-ray diffraction studies were carried out for Cu nanocomplexesFig.4. The Cu nanocomplexes VI, VII and VIII are crystalline in nature. The average crystal sizes of nanocomplexes were calculated by using Debye Scherrer equation [18].

Crystalline size values of Cu nanocomplexesVI, VII and VIII are 24.2 nm, 6 nm and 8.52 nm respectively suggesting that the complexes are in a nanocrystalline phase [19].
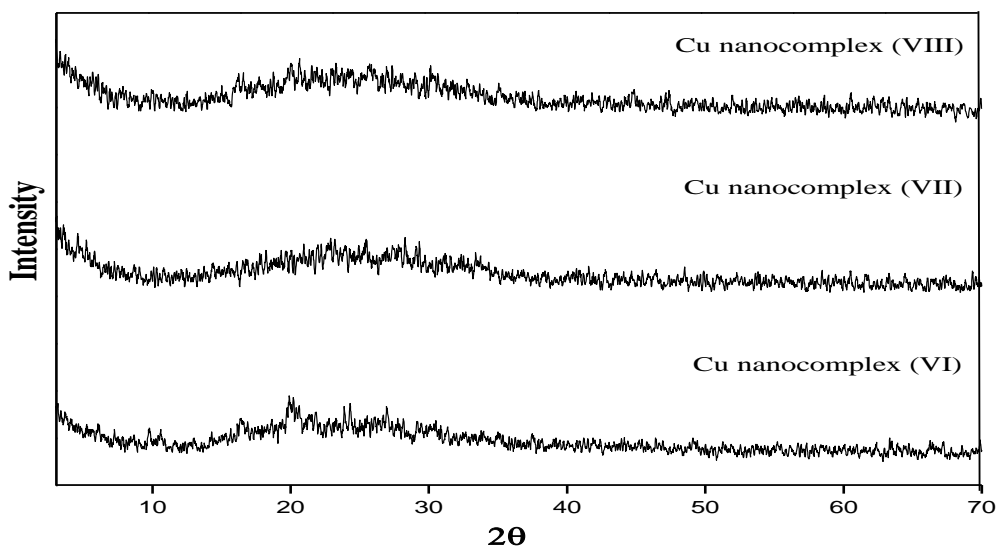
Fig. 4. Powder XRD patterns of the Cu nanocomplexesVI, VII and VIII

III. Result and Discussion

3.1. Elemental Analysis and Molar Conductance of SolidComplexes

Elemental analysis and molar conductance results are collectedin Table 1. From analytical data, the synthesized complexes showed that the metal ions reacted with the ligand in molar ratios 1: 2 (metal: ligand). The results indicated that the synthesized ligand coordinate to metal ion through phenolic oxygen and nitrogen atom of azomethine group. All preparedmetal chelates have Ω_m values within the range (11-22 ohm^{-1} cm^2 mol^{-1}) revealingthe non-electrolytic behavior of complexes, hence all these complexes are neutral [20].

3.2. IR Spectral Studies

The main bands of free Schiff base ligand and its metal complexes were collected in Table 2. The disappearance of υOH phenolic in the IR spectra of metal complexes which are observed at 3446cm^{-1} in the IR of the free ligand, showed that proton displacement from the phenolic -OH group via the metal ion. This is elucidated by the existence of new bands at 523- 548 cm^{-1} in the IR spectra of all metal chelates which are absent in the IR spectra of the free ligand, which could be referred to υM-O bonds [21] . The υC=Nband which observed at 1620 cm^{-1} in the IR of the free ligand are shifted to lower wave numbers by 7-20 cm^{-1} in the IR spectra of all metal complexes under investigation, indicating the coordination of the azomethine nitrogen atoms to the metal ions, which is supported by the existence of new bands in the IR spectra of all metal complexes at 417 - 462 cm^{-1}, these bands would be assigned to υM-N bonds [22]. The IR spectra of the ligand under investigation have two characteristic bands of $\upsilon(SO_2)_{asm.}$ at 1150 – 1157 cm^{-1} and $\upsilon(SO_2)_{sym.}$ at 1089 - 1092 cm^{-1}. These bands appear also at the same position in case of all prepared solid complexes showing that the SO_2 group does not participate in coordination to the metal ion.

3.3.^{1}H-NMR Spectral Studies

A comparative study of the ^{1}HNMR spectra of the CPHPMABS ligand and its Zinc (II) complex (IV) were recorded in DMSO-d6 Fig.5, the following can be pointed out:

i. ^{1}H-NMR (300 MHz, DMSO-d6): 6.59 (d, 1H, J = 8.7 Hz, Ar-H), 6.15 (s, 1H, NH exchangeable with D_2O), 6.97-7.01 (m, 2H, Ar-H), 7.56-7.61 (m, 3H, Ar-H), 8.05 (d, 1H, J = 8.7 Hz, Ar-H), 8.271 (d, 1H, J = 6.9 Hz, Ar-H), 8.33 (s, 1H, H-3pyrazine), 8.36 (s, 1H, H-5pyrazine), 8.96 (s, 1H, CH=N), 12.4 (s, 1H, OH exchangeable with D_2O) .

ii. The signal at δ (8.96) (s, 1H) due to the (-N=CH-) azomethine proton of the Schiff base CPHPMABS shifted downfield in the region of δ (9.99) (s, 1H), confirming the coordination of nitrogen atom of theazomethine (-N=CH-) group with the metal ion.

iii. The peak due to phenolic OH proton originally present at δ 12.4 ppm in free Schiff base ligand CPHPMABS is completely absent from the spectra of Zn(II) complex supporting the bonding takes place through phenolic oxygen atom.
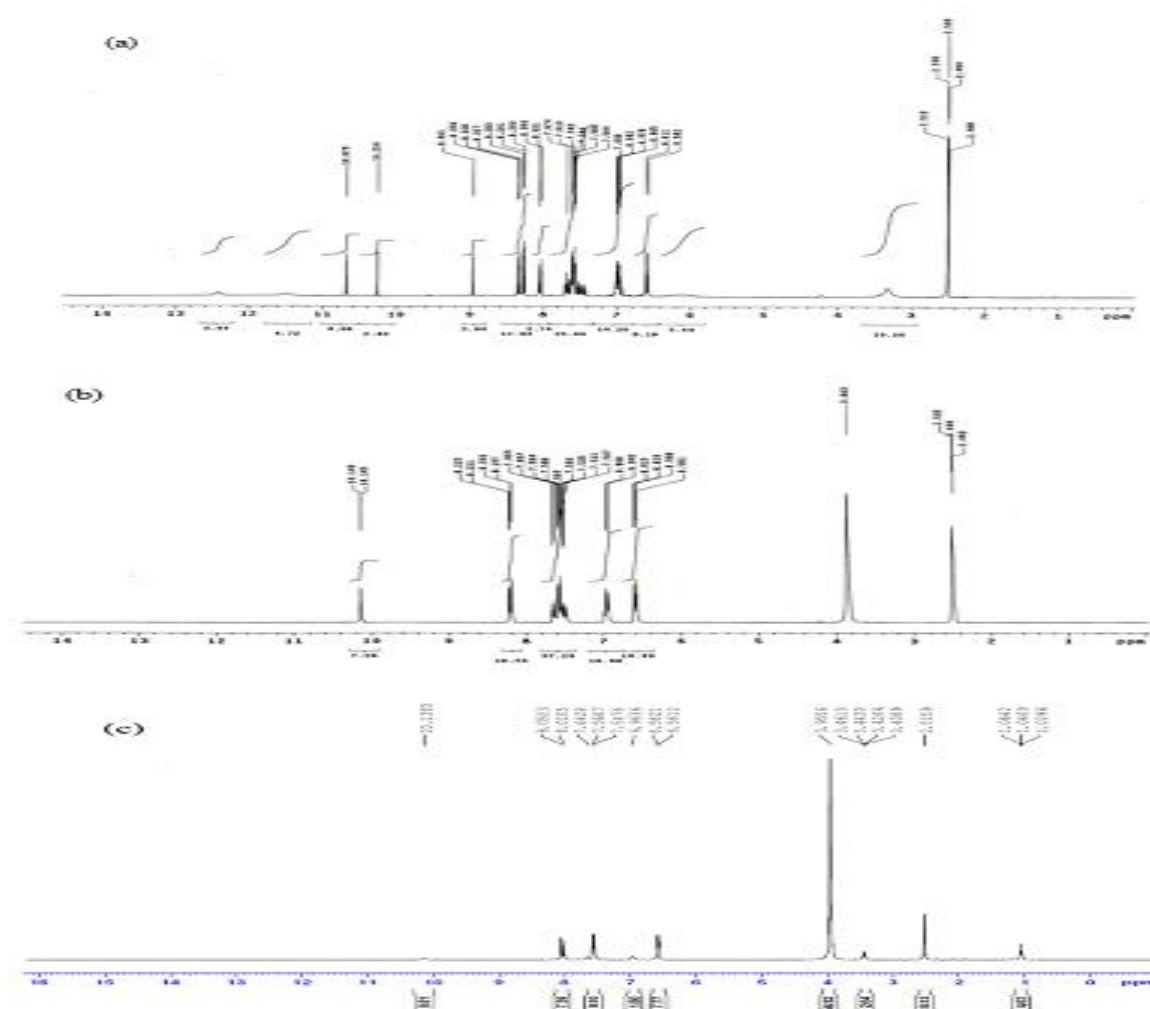
Fig. 5. ^{1}HNMR spectrum of CPHPMABS (HL), (a) with DMSO, (b) with DMSO + D_2O and (c) its Zn II complex.

3.4. Thermal analysis studies

Thermal gravimetric analysis is very important tool to study the stability of the prepared metal complexes, to define whether the water or solvent molecules are inside or outside the coordination sphere in addition to predict a general scheme for the thermal decomposition of these complexes [23, 24].

The TGA-DTG curves of Co(II), Ni(II) and Cu (II) complexes of the CPHPMABS (HL) ligand were carried out from ambient temperature up to 800 °C under N_2 gas flow at heating rate of 10 °C/min as shown in Fig.6.

The TG thermogramof Co(II) complex involves three decomposition steps Scheme 3; a mass loss occurred within the temperature range 29 – 332 °C corresponding to the loss of 7.24% (calcd 7.94%) for two molecules of lattice water and two molecules of coordinated water. At the temperature range 332 – 461 °C another loss of 73.64% (calcd. 28.14%) for $2SO_2$, 2HCl and 2HCN molecules. at the higher temperature range 461 – 800 °C a mass loss of 54.86 % (calcd. 55.63%) corresponding $C_{32}H_{20}N_6O$ as a part of the ligand. then it formsCoO.

$$[Co(C_{34}H_{24}N_8S_2O_6Cl_2)(H_2O)_2]2H_2O$$

Complex (I)
M.wt. = 905.9

-(2 lattice H_2O +
2 coordinate H_2O)   29°C - 332°C
found % (Calcd%)
7.24% (7.94%)

$$[Co(C_{34}H_{24}N_8S_2O_6CL_2)]$$

-(2 SO_2 + 2 HCl + 2 HCN)   332°C - 461°C

27.64% (28.14%)

$$[Co(C_{32}H_{20}N_6O_2)]$$

- $C_{32}H_{20}N_6O$ 461°C -800°C
54.86% (55.63%)

CoO
Residue
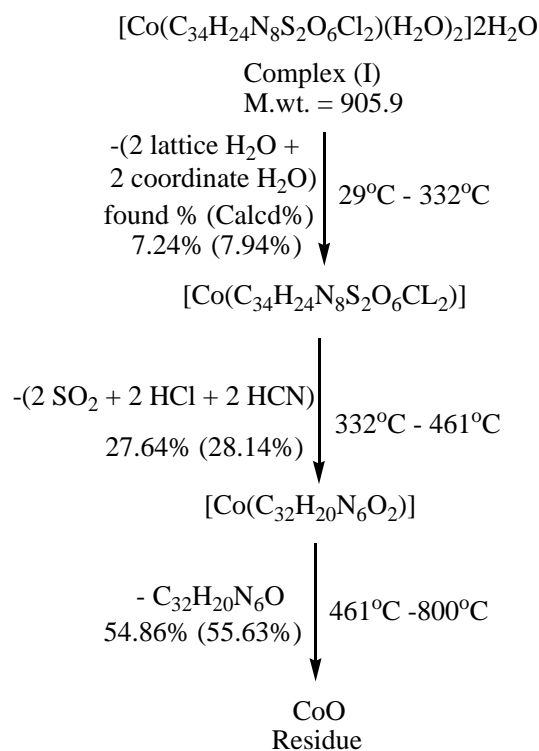
Scheme 3. Proposed thermal decomposition pattern of Co(II) complex

The TG thermogramof Ni(II) complex includes three decomposition steps Scheme 4 ; a mass loss occurred within the temperature range 39 – 200 °C corresponding to the loss of 7.41% (calcd 7.95%) for two molecules of lattice water and two molecules of coordinate water. At the temperature range 200 – 289 °C another loss of 27.53 % (calcd. 28.15%) for 2SO_2, 2HCl and 2HCN molecules At higher temperature range 289 – 800 ˚C a loss of 55.11 % (calcd. 55.65 %) for $C_{32}H_{20}N_6O$ as a part of ligand decomposition, then it forms NiO.

$$[Ni(C_{34}H_{24}N_8S_2O_6Cl_2)(H_2O)_2]2H_2O$$

Complex (II)
M.wt. = 905.6

-(2 lattice H_2O +
2 coordinate H_2O)   39°C - 200°C
found % (Calcd%)
7.41%   (7.95%)

$$[Ni(C_{34}H_{24}N_8S_2O_6CL_2)]$$

-(2 SO_2 + 2 HCl + 2 HCN)   200°C - 289°C

27.53% (28.15%)

$$[Ni(C_{32}H_{20}N_6O_2)]$$

- $C_{32}H_{20}N_6O$ 289°C -800°C
55.11% (55.65%)

NiO
Residue
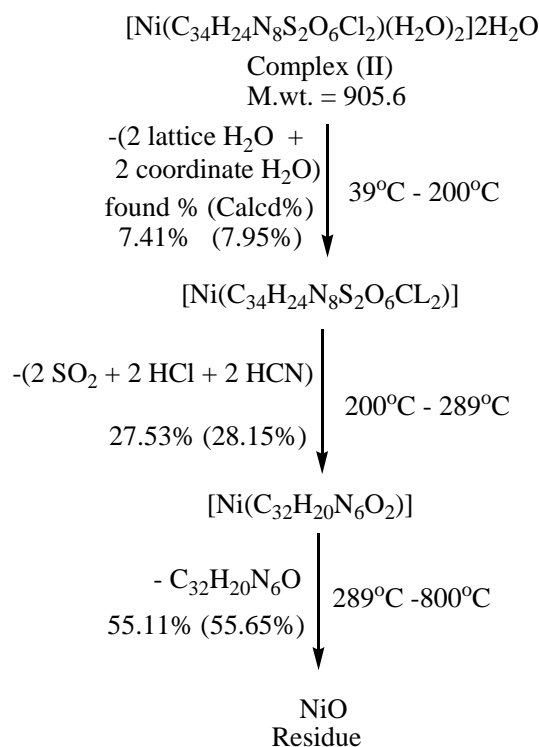
Scheme 4. Proposed thermal decomposition pattern of Ni (II) complex

The TG thermogram of Cu(II) complex involves three decomposition steps Scheme 5 ; a mass loss occurred within the temperature range 41 – 231 ^{o}C corresponding to the loss of 3.92% (calcd. 4.03%) for one lattice water molecule and one molecule of coordinated water. At the temperature range 231.3 – 370 ^{o}C another loss of 27.3% (calcd. 27.56%) for one coordinate water molecule, $2SO_2$, 2HCl and HCN molecule. At higher temperature range 370 – 800 ^{o}C a loss of 59.16% (59.49%) corresponding $C_{33}H_{21}N_7O$ as a part from the ligand, then it forms CuO.

$$[Cu(C_{34}H_{24}N_8S_2O_6Cl_2)(H_2O)_2]H_2O$$

Complex (III)
M.wt. = 892.5

-(lattice H_2O +
coordinate H_2O)   41°C - 231°C
found% (Calcd%)
3.92% (4.03%)

$$[Cu(C_{34}H_{24}N_8S_2O_6Cl_2)(H_2O)]$$

-(coordinate H_2O + 2 SO_2 +
2 HCl + HCN)   231.3^{o}C - 370°C
27.3% (27.56%)

$$[Cu(C_{33}H_{21}N_7O_2)]$$

- $C_{33}H_{21}N_7O$ 370.2^{o}C - 800°C
59.16% (59.49%)

CuO
Residue
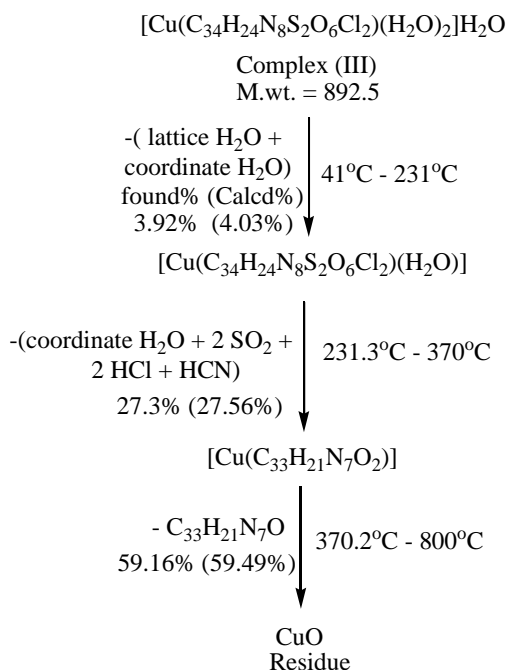
Scheme 5. Proposed thermal decomposition pattern of Cu(II) complex

The order n and activation energy, E* of the decomposition steps for investigated complexes are determined from TGA results by using the Coats-Redfern equation [25]; the thermo kinetic parameters are calculated and listed in Table 3.
From the results, the conclusions are summarized as following:
i. The ΔS^* has a positive value for all the metal chelates. This indicated that the activated complex is less ordered than the reactants and / or the reactions are fast [26].
ii. The positive value of ΔG^* revealed that the free energy of the final residue is higher than that of the initial compound. This shows that all the steps of decompositionare nonspontaneous [27].
iii. The activation enthalpy change has a positive values ΔH^* indicated that the decomposition stages are endothermic.

From the decomposition temperatures of the prepared complexes the thermal stability was deduced in the order:
Ni(II) complex > Cu(II) complex > Co(II) complex
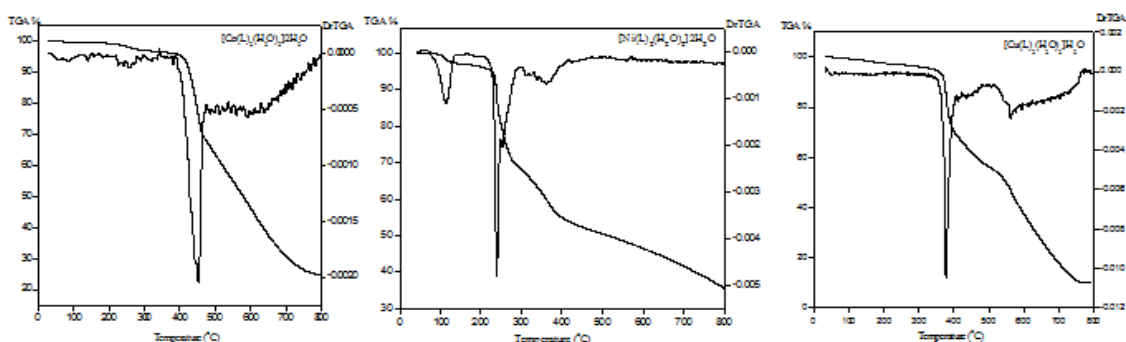
Fig. 6. TGA - DrTGA curves of Co(II), Ni(II) and Cu(II) complexes

3.5. Magnetic Properties

The magnetic moment values were performed at room temperature. The magnetic measurements for Co (II) and Ni (II) complexes showed magnetic moment values of 5.3 and 2.83 B.M. respectively, indicating octahedral environment [28]. The Cu (II) complex exhibits the magnetic moment value of 2.02 BM expected for one unpaired electron suggesting a distorted octahedral geometry [29].

3.6. Electronic Spectral Studies

The electronic spectra of metal II complexes (I – X] are performed in freshly prepared DMF solution (10^{-3} M) at room temperature. The electronic absorption spectra of the Co(II) complex exhibited two bands at 596 and 654 nm corresponding to $^4T_{1g}(F) \rightarrow {}^4A_{2g}(P)$ and $^4T_{1g}(F) \rightarrow {}^4T_{1g}(P)$ transitions indicating octahedral structure[30].

The Ni(II) complexshow two absorption bands, at 642 and 691 nm which refer to $^3A_{2g}(F) \rightarrow {}^3T_{1g}(F)$ and $^3A_{2g}(F) \rightarrow {}^3T_{1g}(P)$ transitions, respectively, in an octahedral environment [31].

The Cu(II) complex have a single broad asymmetric band in the region of 703 nm corresponding to $^2Eg \rightarrow {}^2T_{2g}$ transitions. The broadness of the band is due to dynamic Jahn-Teller distortion. All of these data predicted a distorted octahedral geometry around the Cu(II) ion [32].

The geometrical structure of Cd(II) complex was established from molecular modeling data which gives square planner geometry, table 6 , accordingly the Zn(II) complex posses the same geometrical structural arrangement of Cd(II) complex.

The electronic spectra of Cu nanocomplexes (CTAB) and EtOHshowone peak at 575 and 703nm respectively which differ from the absorption spectrum peak ofprepared Cu nanocomplexes using natural green plants which givestwo peaks at598 and 647nm for Cu nanocomplex(SO)whileCu nanocomplex (MP)shows two peaks at 600 and 649 nm

3.7. ESR Spectra of Cu(II) Complexes

X-band ESR spectra of Cu (II) complex namely $[Cu(L)_2(H_2O)_2]H_2O$ is performed at room temperature as shown in Fig.7.The g_{eff}values of Cu(II) complex is 2.085. From g_{eff} values and shape of ESR signals, Cu (II) complex under investigation suggested to have distorted octahedral geometry.The g-value of the Cu (II) complex showed that $g_{\parallel} > g\perp$ which indicated that the unpaired electron in the dx^2-y^2 orbital is predominantly [33] giving $^2B_{1g}$ as the ground state. The result showed that the $g_{\parallel}$ values are > 2.0023 for complexes. This indicates that the metal-ligand bonding in this Cu (II) complex is covalent character [34]. The g-values related by this expression, $G = (g_{\parallel} - 2) / (g\perp - 2) = 4$, which measure the exchange interaction between the Cu (II) centers in the solid. If G value is more than 4, the exchange interaction between the Cu (II) centers is negligible, while G is lower than 4 a considerable exchange interaction is showed in the solid complex. The calculated G values for Cu(II) complex is 1.98 which proposed a Cu-Cu exchange interaction [35].
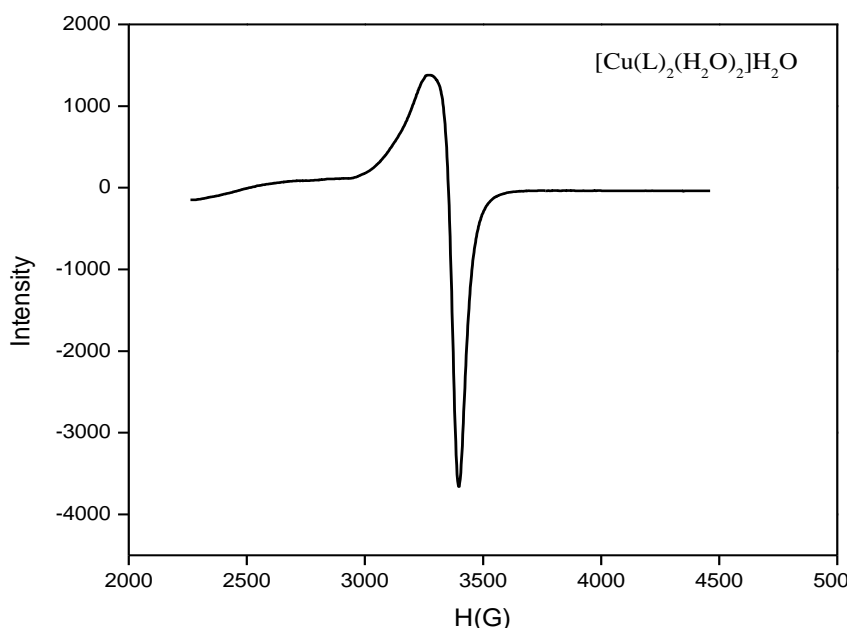
Fig.7. X-band ESR spectra of Cu(II) complex

IV. Molecular modeling studies of ligand CPHPMABS and its Cd II) complex

The geometrical structures of the synthesized ligand and its Cd (II) complex are optimized using Material Studio program and the molecular modeling of free ligand CPHPMABSand its Cd (II) complex shown in Figs. 8 and 9respectively.

-The LUMO - HOMO energy gap (ΔE) is an important way to study the stability of metal complexes. While the LUMO – HOMO energy gap decreases, the interactions between the reacting species will be stronger and lead to increase the stability of the formed metal complexes [36]. The values of ΔE showed that the ligand under study have high tendency to bind with the metal ions [37].

- The order of Egap (eV) that measures the reactivity of the Schiff base ligand and its Cd(II) is: Cd(II) complex > Free ligand CPHPMABS , Fig. 10.

- Additional parameters, such as separation energy, ΔE, electrophilicity index (χ), chemical potential (pi), absolute hardness (η), absolute softness (σ) and additional electronic charge (ΔN$_{max}$) have been calculated [38, 39] and listed in Table4.

- Absolute hardness (η) and softness (σ) are important properties to measure the molecular stability and reactivity. Therefore, it is observed that the ligand CPHPMABS (HL), with proper σ values have a good effectively inclination to chelate metal ions.

- The reactivity index is used to measure the stabilization in energy when a system gains an extra electronic charge (ΔN$_{max}$) from the environment. electrophilicity index (χ) is a positive, definite quantity and the direction of the charge transfer is completely determined by the electronic chemical potential (pi) of the molecule because an electrophile is a chemical species able to accept electrons from the environment and its energy must decrease upon accepting electronic charge. Hence, the electronic chemical potential must be negative as indicating in the obtained values in Table4.
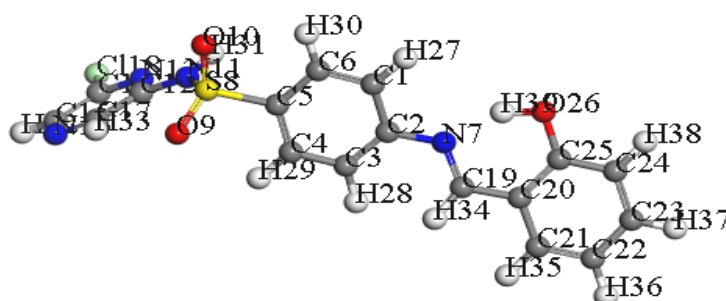
Fig.8. 3D modeling structure of the ligand CPHPMABS
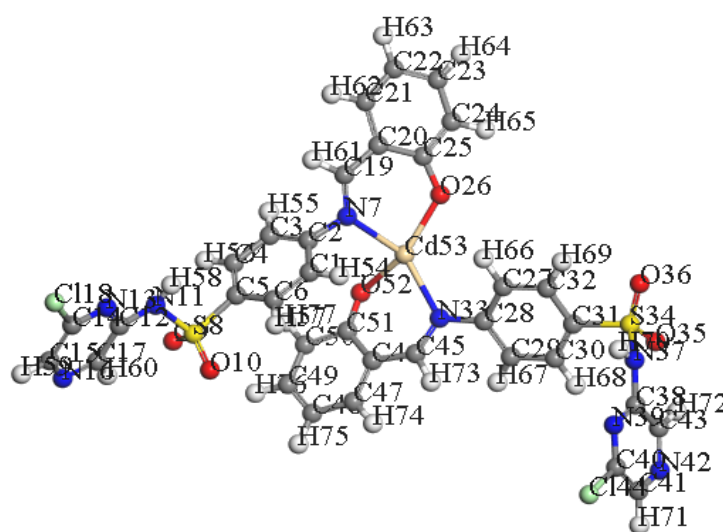
Fig. 9. 3D modeling structure of the Cd(II) complex

(a)	(b)
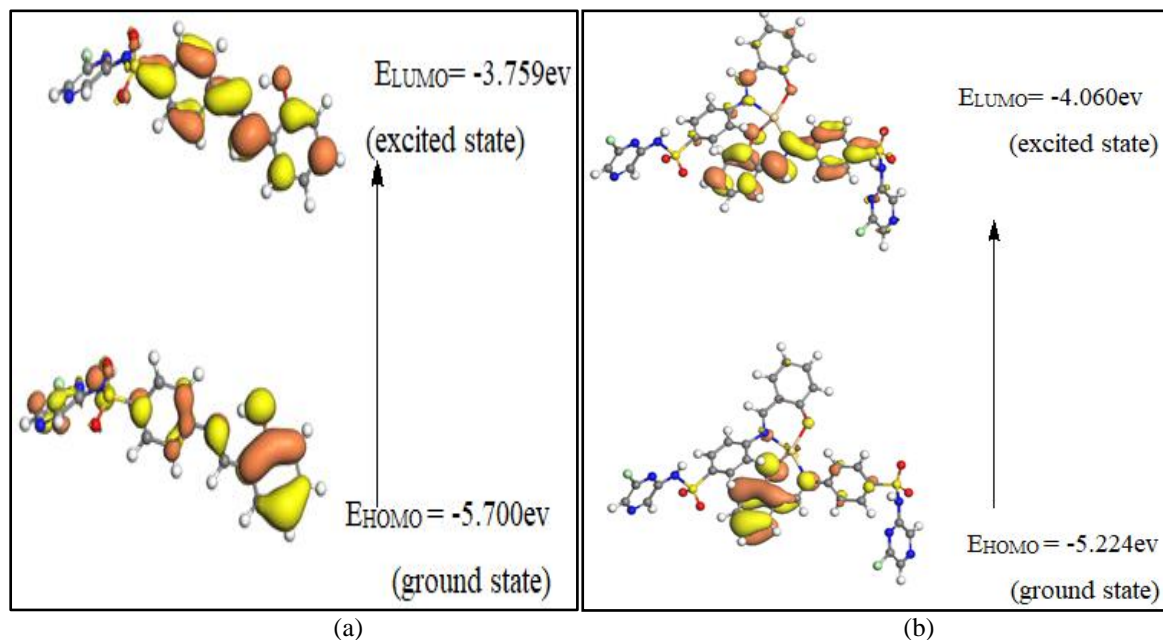
Fig.10.3D plots frontier orbital energies using DFT method for (a) Schiff base ligand and (b) its Cd(II) complex

4.1. Bond Lenhgth and Bond angle

Bond lengths and bond angles of CPHPMABS Schiff base ligand and its Cd(II) complex are calculated in Tables5 and 6. From theseresults, the following can be pointed out:

1. The optimized $(C=N)_{azomethine}$ bond length elongated due to its coordinate in complex.

2. The $C(25) – O(26)_{phenolic}$ bond lengths becomes longer slightly in Cd(II) complex due to the coordination via O(26) that is formed on deprotonation of OH phenolic group. Also, The $N(7) -C(19)_{azomethene}$ bond lengths elongated in complexes due to the coordination takes place through N (7) of azomethene group.

3. There is elongation in C– O bond distance in Cd(II) complex as a result of formation of the M-O bond which cause weakness in C – O bond [38].

4. The bond angles of Schiff base ligands are changed somewhat upon coordination; the largest change affects C(20)-C(19)-N(7) angle which are increased or decreased on complex formation as a result of bonding [38].

5. The bond angles in Cd(II) complexes fall in the range of square planner geometry predicting Sp^2d hybridization.

6. The bond angles within the sulphaclozine moiety do not change but the angles around the Cd(II) changed as a consequence of coordination with the ligand (CPHPMABS).

V. Biological Activities

5.1. Antitumor activity

Schiff base ligand (CPHPMABS) and its Cu nanocomplexesIII, VI, VII and VIII are screened as an antitumor agent towards Hepatocellular carcinoma cell line (HepG-2) with cis-platin. IC_{50} values were calculated and the results were listed in Table 7.

$IC_{50}$is the inhibition concentration of a substance that inhibit 50%of the tumor cell. The results of antitumorindicate that Cu nanocomplex IIIis more active than free ligand (CPHPMABS). This revealed the increasing of antitumor activity upon coordination. AllCu nanocomplexesIII, VI, VII and VIII with IC_{50} value of 5.94, 3.79, 14.6 and 16.37 µg/ml respectively, show high antitumor activity, this nanocharacter increased the antitumor activity due to easily penetration of Cu nanocomplex into tumor cell.The results of antitumor activity indicate nanocomplexVIis the highest cytotoxicity compound.

The order of antitumor activityas shown in Fig. 11 is:

Cisplatin ≈ Cu nanocomplexVI>Cu nanocomplexIII > Cu nanocomplex VII > Cu nanocomplex VIII >free ligand (CPHPMABS).

From above resultswe can conclude that antitumor activity increase by decreasing particle sizes of nanocomplexes due to easily penetration of these compoundsinto tumor cell.

These results have widened the scope of developing these compounds as promising antitumor drugs.
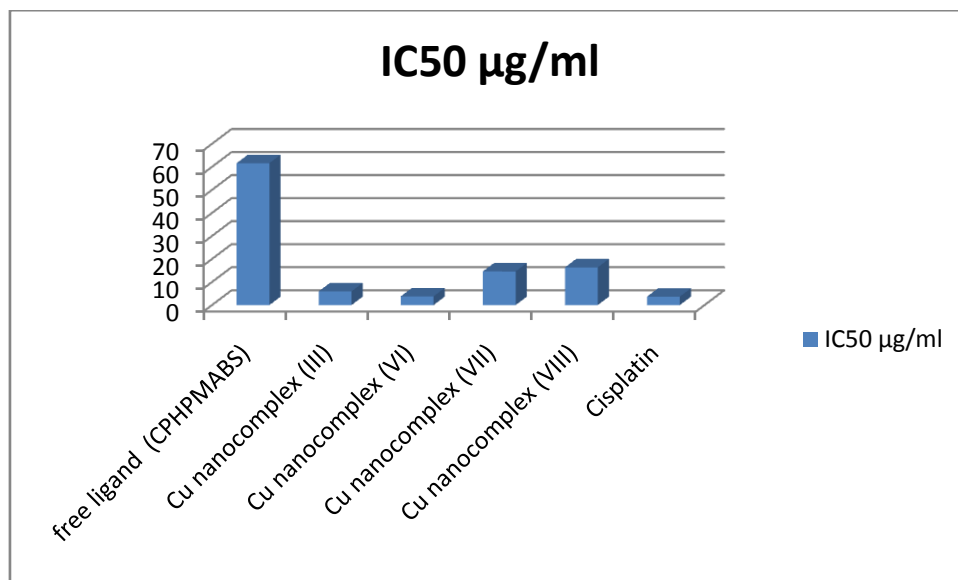
Fig. 11. In vitro antitumor activities of Schiff base ligand CPHPMABS and its Cu nanocomplexes on Hepatocellular carcinoma cell line (HepG-2).

5.2. Antibacterial and Antifungal Assays

The biological activities of synthesized ligand(CPHPMABS) , its complexes (I - V) and Cu nanocomplexes (VI, VII and VIII) are tested for their antibacterial and antifungal properties using the agar diffusion method in DMF solvent against *Escherichia coli*, *Bacillus subtilis*and*Salmonella typhi*bacteria, *Staphylococcus aureus,Candidaalbicans*and *Aspergillusfumigatus*fungi. The results of biological activities are presented in Table8.A comparative study of the free ligand (CPHPMABS) and its metal chelates revealed that most complexes have higher antimicrobial activity than the freeligand (CPHPMABS). The greatestactivities of the metal chelates wereelucidatedbyTweedy's chelation theory [40] and Overtone's concept [41]. All these metal chelates also stopped the respiration process of the cell and thereforeblocked the synthesis of the proteins and preventing the growth oforganism. Also, the formation of a hydrogen bond between the azomethine group and the active center of the cell, accordingly, interference with the normal cell processes. Generally, metal chelates are more active than free ligand (CPHPMABS) because these metalcomplexes may act as a vehicle for the activation of ligand the principle cytotoxic species [42]. Cu nanocomplexVII indicated higher antimicrobial activity than the free ligand (CPHPMABS) and its complexes, this is due to its higher surface to volume ratio which can interact with other particles easily and increase its antimicrobial efficiency [43].

Generally, the antimicrobial activity orders are:
Cu nanocomplexVI> Cu nanocomplexVIII > Cu nanocomplexVII>Cu(II) nanocomplex III> Cd(II) complex V > Co(II) complex I > Zn(II) complex IV > Ni(II) complex II>free ligand (CPHPMABS) as shown in the Fig. 12.
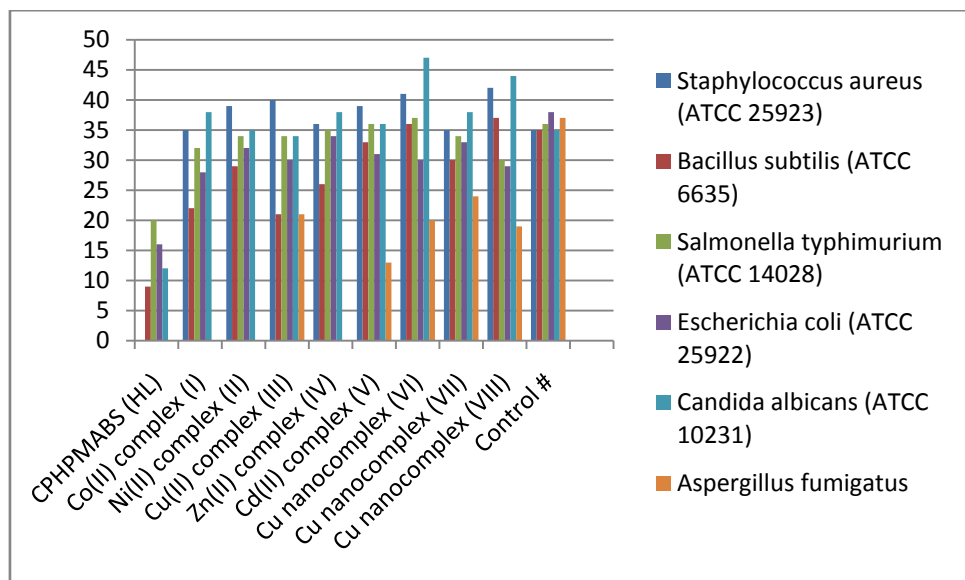
Fig. 12.Antimicrobial and antifugi activity towards ligand CPHPMABS and its metal complexes.

5.3. The molecular docking studies

Carbonic anhdrase enzymes are found in the many tissues perform biochemical function [44]. They can be used as drugs because of these severalinhibitors [45]. They are used as target for anticancer,antipain, antiglaucoma,anticonvulsant, antiobesity,and anti-infectivedrugs. In addition to they are recommended for the treatment ofsome diseases such as obesity, cancer and Alzheimer's [46].

So that, docking simulations were performed to study the binding pattern of the preparedligand (CPHPMABS) and its Cunanocomplex IIIin the active site of the target carbonic anhydrase CA II Fig.13, and the results are collected in Table 9. Carbonic anhydrases use zinc as a metal cofactor to catalyze the reversible inter-conversion of carbon dioxide and bicarbonate ion [47]. Docking setup was validatedby self-docking of the co-crystallized ligand (acetazolamide) in the nearness of the binding site of the enzyme CA II (PDB ID: **3HS4**) [47],Fig. 14.

The ability of the Schiff base ligand and its Cu nanocomplex to interact with the key amino acids & Zn^{+2}in the binding site showed good activity as indicated by their docking pattern and docking scores compared to that of acetazolamide. The docking study revealed that Cu nanocomplex is possibility inhibitors of cancer causing receptors. This docking study revealed that developing these sulphaclozine compounds as antitumor drugs.
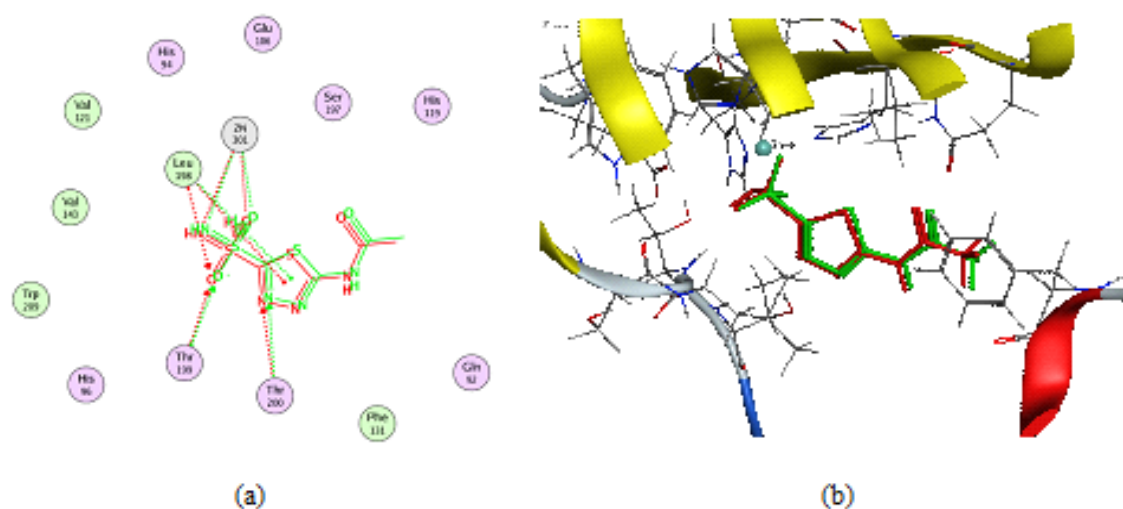
Fig.13.a) 2D representation and b) 3D representation of the superimposition of the co-crystallized (red) and the docking pose (green) of acetazolamide in CAII binding site with RMSD of 0.2981 A°.

(a)

(b)
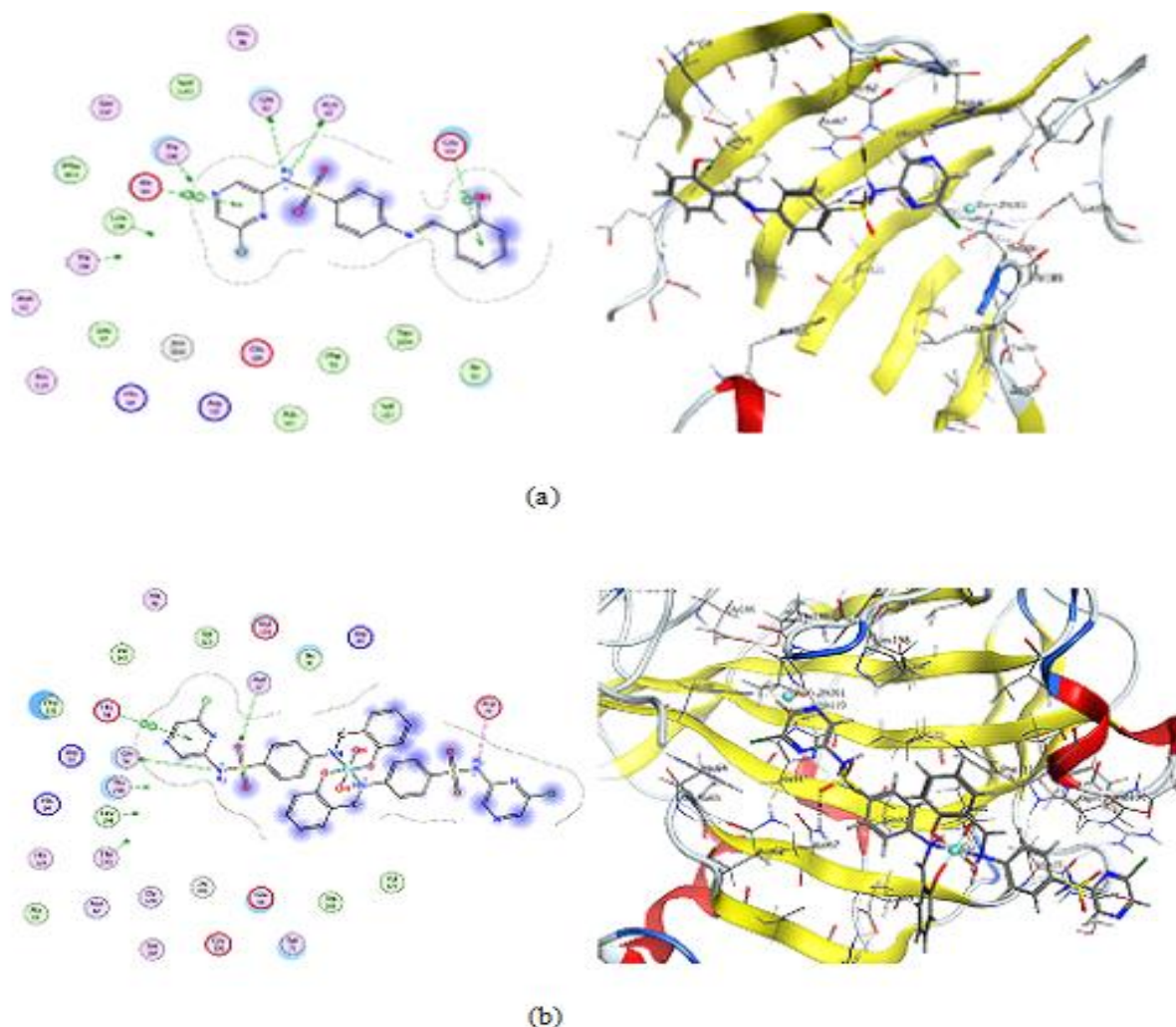
Fig. 14. (a) 2D & 3D diagrams of Schiff base ligand(CPHPMABS) showing its interaction with the CAII binding site and (b) 2D & 3D diagrams of Cu(II) nanocomplex III showing its interaction with the CAII binding site.

VI. Electrical Conductivity Studies

The variation of ac-conductivity with the temperature for the Cu nanocomplexes III and VI under study in the frequency range of $100 - 8 \times 10^6$ Hz is shown in Fig.15. The conductivity increases with the temperature. Generally, the temperature dependence of conductivity for the studied compounds follows the semiconducting behavior which playsan important role in energy conversion and storage through photovoltaic effect, light-emitting nanodevices, water splitting and solar fuels [48].

This is due to the increase in each of the concentration of charge carriers and may be attributed to the increase in charge mobility because thermal energy of the molecules increased with temperature. Therefore, the bound charges have been converted into the mobile charges. The data obtained also show that the Ac-electrical conductivity of Cu nanocomplexVI (particle size 8.5 nm) is higher than Cu nanocomplex III(particle size 14 nm), these can be attributed to the particle size as increased will decrease the ionic mobility.

The activation energy E_a has been calculated from the slopes of $\ln\sigma_{ac}$ versus $1000/T$ plots, by using the Arrhenius's equation [49]

$$\sigma_{ac} = \sigma_0 \exp\left(-E_a / K_b T\right)$$

The values of E_a were calculated at frequency 1000 Hz and given in Table 10.
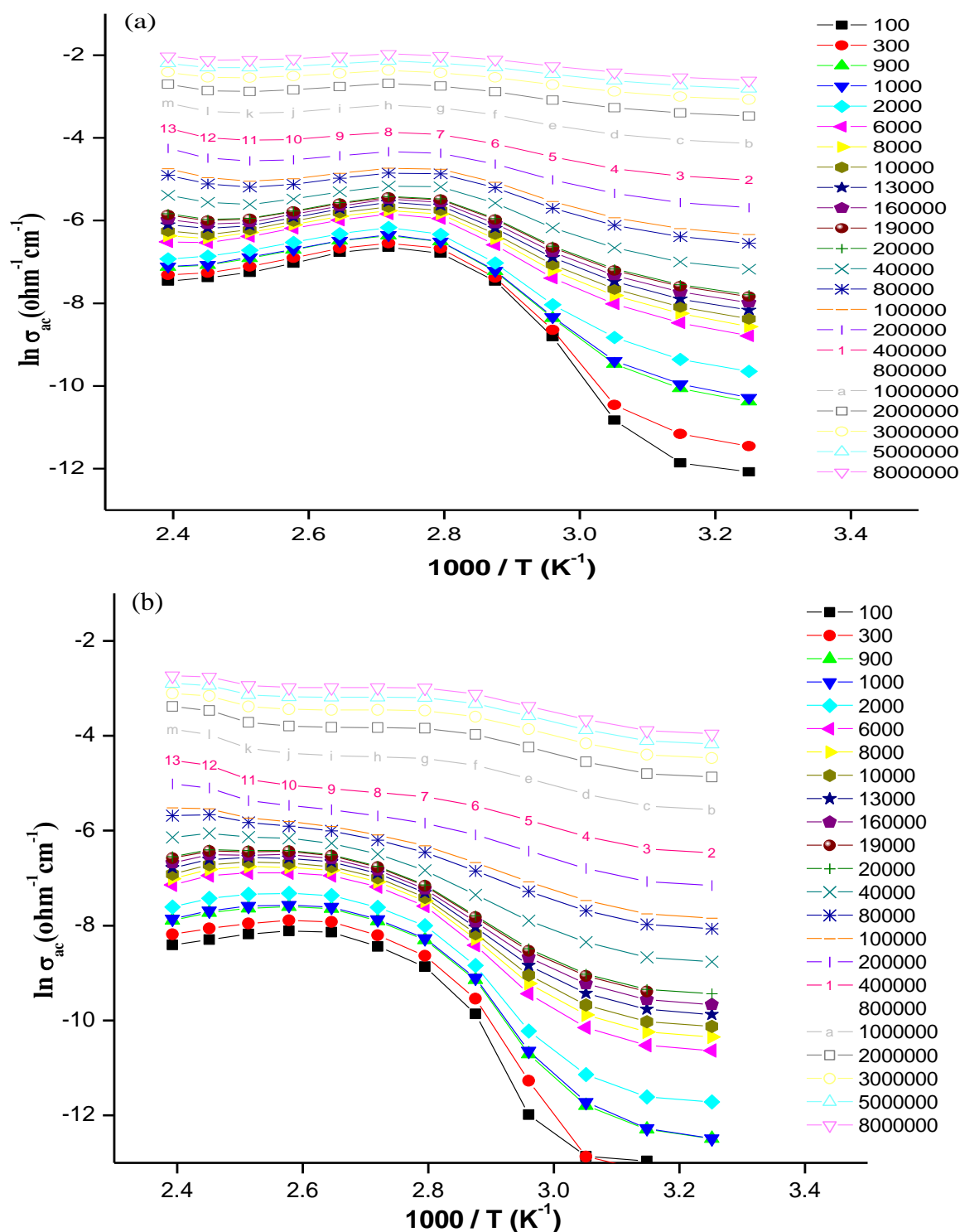
Fig. 15. Effect of temperature on AC-electrical conductivity for (a) Cu nanocomplex III and (b) Cu nanocomplex VI.

VII. Conclusion

New Cu nanocomplexes have been synthesized and characterized. These compounds have a great interest recently due to unique physical and chemical properties and low cost of preparation in which have great applications as antimicrobial and anticancer materials. The docking study showed that metal complex is potential inhibitors of cancer causing receptors. This study has widened the scope of developing sulphaclozine compound and its metal (II) chelates as promising antitumor drugs. The newly prepared Schiff base ligand (CPHPMABS) acted as a mono-negative bidentate ligand. The metal ion coordinated through the phenolic oxygen atom and azomethine nitrogen atom. The electrical conductivity studies show semiconductor nature for

Cu nanocomplexes which can be used as light-emitting nanodevicesand solar fuels.From the above obtained results of thermal and elemental analyses, conductance and magnetic moment measurements as well as different spectral studies, the proposed structures of the metal chelates under investigation can be formulated as Schemes (6 and 7).

Complex (I)	M = Co^{+2}	y = 2H$_2$O	X=
Complex (II)	M = Ni^{+2}	y = 2H$_2$O	X= ,, ,,
Complex (III)	M = Cu^{+2}	y = H$_2$O	X= ,, ,,
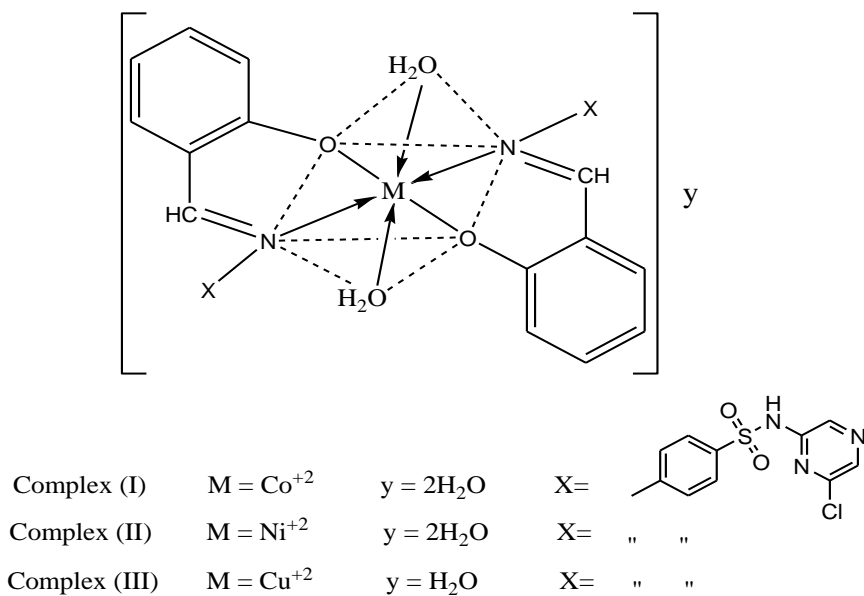
Scheme 6 proposed structure of metal complexes

Complex (IV)	M = Zn^{+2}	X =
Complex (V)	M = Cd^{+2}	X = ,, ,,
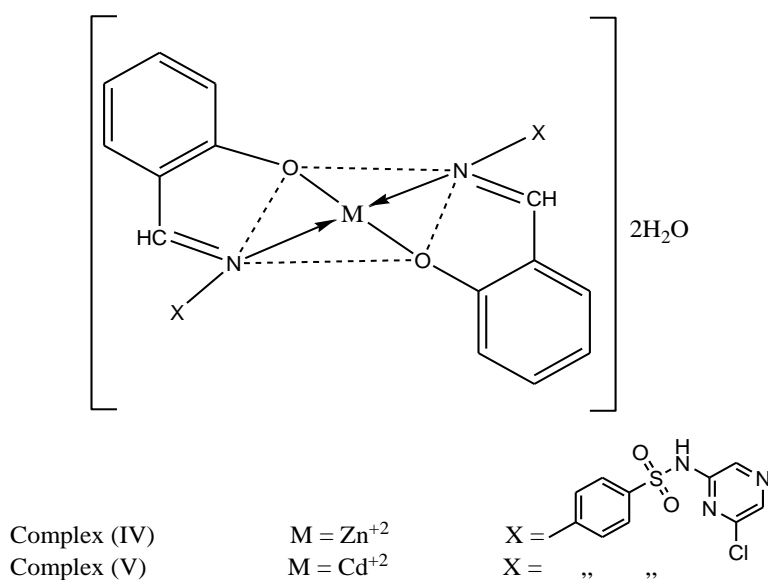
Scheme 7 proposed structure of metal complexes

Table 1. Analytical and Physical data of the metal complexes of CPHPMABS (HL) ligand

No.	Complex	Colour	m.p. (°C)	M. Wt.	Elemental analysis, found % (calcd %)					Ω_m (ohm^{-1} cm^{2}mol^{-1})
					% C	% H	% N	% S	% M	
I	[Co(L)₂(H₂O)₂] 2H₂O	Brick red	>300	905.9	45.15 (45.04)	3.61 (3.53)	12.53 (12.36)	6.85 (7.06)	6.93 (6.50)	22
II	[Ni (L)₂(H₂O)₂] 2H₂O	Pale green	>300	905.6	44.95 (45.05)	3.43 (3.53)	12.02 (12.36)	6.83 (7.06)	6.12 (6.47)	15
III	[Cu(L)₂(H₂O)₂] H₂O	green	280	892.5	45.31 (45.71)	3.21 (3.36)	12.18 (12.54)	7.43 (7.17)	7.65 (7.11)	11
IV	[Zn(L)₂] 2H₂O	Yellow	275	876.3	46.25 (46.56)	3.42 (3.19)	12.49 (12.78)	6.96 (7.30)	7.87 (7.45)	17.2
V	[Cd (L)₂] 2H₂O	Pale yellow	>300	923.4	44.58 (44.18)	3.27 (3.03)	11.97 (12.13)	6.46 (6.93)	11.84 (12.17)	14.9

Table 2. Important IR bands and their assignment for CPHPMABS (HL) ligand and its metal(II) complexes

No. Compond		IR Spectral bands (cm^{-1})								
		υ(OH) (H₂O/EtOH)	υ(OH) phenolic	υ(C=N) aliphatic	υ(C=N) ring	υ(SO₂)$_{asm}$	υ(SO₂)$_{sym.}$	ρ(H₂O)	υ(M-O)	υ(M-N)
	CPHPMABSHL	-------	3446	1620	1591	1157	1092	----	-----	-----
I	[Co(L)₂(H₂O)₂] 2H₂O	3431	------	1610	1590	1157	1091	670	538	430
II	[Ni (L)₂(H₂O)₂] 2H₂O	3419	------	1616	1590	1155	1093	664	545	417
III	[Cu(L)₂(H₂O)₂] 2H₂O	3451	------	1607	1591	1157	1090	650	525	450
IV	[Zn(L)₂] 2H₂O	3430	------	1610	1591	1153	1090	683	548	419
V	[Cd (L)₂] 2H₂O	3461	-----	1600	1590	1150	1089	665	523	462

Table 3. Thermodynamic activation parameters of the decomposition of some complexes of CPHPMABS ligand

No.	Complex	Step	n	r	Thermodynamic activation parameters				
					E* (KJmol-1)	ΔH* (KJmol-1)	A (S-1)	ΔS* (KJmol-1K-1)	ΔG* (KJmol-1)
I	[Co(L)₂(H₂O)₂] 2H₂O	1st	0.5	0.992	0.032	0.669	0.127	0.088	7.13
		2nd	0.33	0.993	0.146	1.981	11.6 x 10⁶	0.054	11.96
		3rd	0.6	0.996	0.018	3.737	3.8 x 10⁻⁴	0.150	64.42
II	[Ni (L)₂(H₂O)₂] 2H₂O	1st	0.5	0.996	0.108	0.805	6.35 x 10⁹	0.130	13.82
		2nd	1	0.991	0.114	1.88	92.2 x 10⁶	0.072	15.45
		3rd	0.66	0.998	0.006	2.97	5.5 x 10⁻⁵	0.165	56.26

III	[Cu(L)₂(H₂O)₂] H₂O	1st	0.66	0.983	0.025	0.415	0.0728	0.089	4.322
		2nd	0	0.992	0./046	3.12	0.976	0.084	28.96
		3rd	0.5	0.991	0.0004	4.66	1.29×10^{-6}	0.199	107.68

Table 4. (LUMO– HOMO) energy gap (ΔE), the quantum chemical parameters of the CPHPMABS (HL) Ligand with its Cd(II) complex.

No.	Compound	HOMO	LUMO	ΔE	χ	η	σ	Pi	ΔNmax
	CPHPMABS (HL)	-5.700	-3.759	1.941	4.729	0.970	1.0309	-4.729	4.8752
V	[Cd (L)₂] 2H₂O	-5.224	-4.06	1.164	-4.642	0.582	1.7182	4.642	7.9759

Table 5. Calculated bond lengthes of the (CPHPMABSHL) ligand and some of its Cd complex

No.	compound	Bond C-O	Length (Aº)	Bond C=N	Length (Aº)
	CPHPMABS (HL)	C(25) – O(26)	1.354	N(7) - C(19)	1.306
V	[Cd (L)₂] 2H₂O	C(25) – O(26)	1.397	N(7) - C(19)	1.318

Table 6. Calculated bond angles CPHPMABS(HL) ligand with its Cd(II) complex.

Compound	Angle of C-C-N	Degree(º)	Angle of O-C-C	Degree (º)	Angle of C-N-C in sufaclosine moiety	Degree (º)	Angle around metal ion	Degree(º)
CPHPMABS (HL)	C(20)-C(19)-N(7)	121.2	O(26)-C(25)-C(24)	119.9	C(14)-N(13)-C(12)	116.1	----	----
[Cd (L)₂] 2H₂O	C(20)-C(19)-N(7)	128.8	O(26)-C(25)-C(24)	116.7	C(14)-N(13)-C(12)	116.3	O(52)-Cd(53)-N(7)	92

Table 7. Cytotoxicity in vitro of of the Schiff base CPHPMABS HL and its Cu nanocomplexes on Hepatocellular Carcinoma cell line

No.	Compound	IC₅₀ µg/ml
	CPHPMABS (HL)	61.6
III	Cu complex	5.94
VI	Cu nanocomplex	3.79
VII	Cu nanocomplex	14.6
VIII	Cu nanocomplex	16.37
	Cisplatin	3.67

Table 8. Antibacterial and antifungi of Schiff base ligand CPHPMABS (HL), its metal complexes and its Cu nanocomplexes

		Mean* of zone diameter, nearest whole mm.					
		Gram - positive bacteria		Gram - negative bacteria		Yeasts and Fungi**	
No.	compound	*Staphylococcus aureus* (ATCC 25923)	*Bacillus subtilis* (ATCC 6635)	*Salmonella typhimurium* (ATCC 14028)	*Escherichia coli* (ATCC 25922)	*Candida albicans* (ATCC 10231)	*Aspergillusfu migatus*
	CPHPMABS (HL)	-	9	20	16	12	-
I	[Co(L)₂(H₂O)₂] 2H₂O	35	22	32	28	42	-
II	[Ni (L)₂(H₂O)₂] 2H₂O	39	29	34	32	35	-
III	[Cu(L)₂(H₂O)₂] H₂O	40	21	34	30	34	21
IV	[Zn(L)₂] 2H₂O	36	26	35	34	38	-
V	[Cd (L)₂] 2H₂O	39	33	36	31	36	13
VI	Cu nanocomplex	41	36	37	30	47	20
VII	Cu nanocomplex	35	30	34	33	38	24
VIII	Cu nanocomplex	42	37	30	29	44	19
	Control #	35	35	36	38	35	37

Table 9. Details of interaction of Schiff base ligand and its Cu nanocomplex III with enzyme

Compound	S (kcal/mol)	Amino acids	Interacting groups	Type of interaction
CPHPMABS HL	-5.2352	Asn67	NH (S)	H-bond (donor)
		Glu69	Phenyl	Arene-H
		Gln92	NH (S)	H-bond (donor)
		His94	Pyrazine	Arene-Arene
Cu nanocomplex (III)	-7.0002	Asn67	O (S)	H-bond (acceptor)
		Asp72	NH (S)	H-bond (donor)
		Gln92	NH (S)	H-bond (acceptor)
		His94	Pyrazine	Arene-Arene
AZA	-9.6180	-----	O (S)	Metal complex (Zn)
		-----	NH (S)	Metal complex (Zn)
		Leu198	Thiadiazole	Arene-H
		Leu198	O (S)	H-bond (acceptor)
		Thr199	O (S)	H-bond (acceptor)

Table 10. The electrical conductivities (Ω^{-1} cm^{-1}) and activation energy (eV) of Cu nanocomplexes

Compounds	Temperature range K	Electrical conductivities (σ_{Ac})	Activation energy (Ea)
Cu nanocomplex (III)	307 – 357.8	2.47×10^{-2}	1.2×10^{-19}
Cu nanocomplex (VI)	307 – 357.8	1.6×10^{3}	1.045×10^{-19}

References

[1]. N. Sahu , S. Mondal, K. Naskar, A. Das Mahapatra,S. Gupta, A. M.Z. Slawin, D. Chattopadhyay, C. Sinha,Spectroscopic characterization, antimicrobial activity and molecular docking study of novel azo-imine functionalized sulphamethoxazoles, J. Mol. Struct. 2018, 1155, 152-164.

[2]. D. F. Sallam, T. M. A. Ismail, A. M. Tawfik, S. M. Abu-El-Wafa, Novel Schiff base ligand N-(6-chloropyrazin-2-yl)-4-{[(E)-(2-hydroxynaphthalen-1- yl)methylidene] amino} benzenesulfonamide (CPHNMABS), its metal(II) chelates and nanocomplexes: Synthesis, structural characterization, DNA, antitumor, docking studies, antimicrobial activity and conductivity studies, IOSR Journal of Applied Chemistry(IOSR-JAC)**2020**, 13, 6 – 24.

[3]. S. S. Hamdani, B. A. Khan, S. Hameed, F. Batool , H. N. Saleemc , E. U. Mughald , M. Saeed,Synthesis and evaluation of novel S-benzyl- and S-alkylphthalimideoxadiazolebenze-nesulfonamide hybrids as inhibitors of dengue virus protease, Bioorg. Chem. **2020**, 96 103567.

[4]. F. A. Saad, H. A. El-Ghamry, M. A. Kassem, Synthesis, structural characterization and DNA binding affinity of new bioactive nano-sized transition metal complexes with sulfathiazole azo dye for therapeutic applications, Appl. Organometal. Chem., **2019** e 4965.

[5]. P. Forgacs, N. L. Wengenack, L. Hall, S. K. Zimmerman, M. L. Silverman, G. D. Roberts, Tuberculosis and Trimethoprim-Sulfamethoxazole, Antimicrob. Agents Chemother. 2009, 53(11): 4789–4793.

[6]. C. M. Sharaby, M. F. Amine, A. A. Hamed, Synthesis, structure characterization and biological activity of selected metal complexes of sulfonamide Schiff base as a primary ligand and some mixed ligand complexes with glycine as a secondary ligand,*J. Mol. Struct.*, **2017**, 1134, 208 – 216.

[7]. G. Valarmathy , R. Subbalakshmi, R. Sumathi, R. Renganathan, Synthesis of Schiff base ligand from N-substituted benzenesulfonamide and its complexes: Spectral, thermal, electrochemical behavior, fluorescence quenching, in vitro-biological and in-vitro cytotoxic studies, J. Mol. Struct. **2020**, 1199, 127029,

[8]. A. Agudo-López, E. Prieto-García, J. Alemán, C. Pérez, C. V. Díaz- García, L. Parrilla- Ortuño, Mechanistic added value of a trans-Sulfonamide-Platinum-Complex in human melanoma cell lines and synergism with cis-Platin, *Mol. Cancer* 2017,16(1), 45.

[9]. S. Rostamizadeh, Z. Daneshfar, H. Moghimim, Synthesis of sulfamethoxazole and sulfabenzamide metal complexes; evaluation of their antibacterial activity, European Journal of Medicinal Chemistry **2019**, 171, 364 -371.

[10]. V. Gomathi , R. Selvameena, Spectroscopic investigation, fluorescence quenching, in vitro antibacterial and cytotoxicity assay of Co(II) and Ni(II) complexes containing 4-((3-ethoxy-2-hydroxy benzylidene)amino)-N-(pyridin-2-yl)benzenesulfonamide, Inorg. Chim.Acta**2018**, 480, 42–46

[11]. A. Pontorieroa , N. Mosconi , L. Monti , S. Bellú , P. A.M. Williams , M. Raimondi , B. Lima , G. E. Feresin , B. Nerli , M. Rizzotto, Synthesis, characterization and biological studies of a cobalt(III) complex of sulfathiazole, Chemico-Biological Interactions, **2017**, 278, 152–161.

[12]. A. I. Vogel, A Text Book of Quantitative Inorganic Analysis, 3rd ed., Longman ELBS, London**1968**.

[13]. T. M.A. Ismail, H. M.A Soliman, S. M. Abu-El-Wafa, D. F. Sallam,Synthesis, Characterization, 3D Modeling, Nano Structures, Anti- Microbial and-Anti Cancer Activity Studies of Metal (II) Chelates of a Novel Bioactive Schiff Base Ligand Derived from Sulphaquinoxaline J. Chem. Bio. Phy. Sci. Sec. A, **2016**, 6, 751-776.

[14]. T. M. Ismail, M. A. EL Ghamry, S. M. Abu-El-Wafa, D. F. Sallam, Synthesis, Characterization, 3D Modeling, Biological Activities of Some Metal Complexes of Novel SulphaDrugSchiff Base Ligand and Its Nano Cu ComplexModern Chemistry, **2015**, 3, 18 – 30.

[15]. A. Athawale, M. Kumar ,Synthesis of CTAB–IPA reduced copper nanoparticles, Materials Chemistry and Physics**2005**, 91(2):507-512.

[16]. M. F. Zayed, W. H. Eisa, A. A. Shabaka, Malvaparviflora extract assisted green synthesis of silver nanoparticles Spectrochim. ActaPart A, **2012**, 96, 423.

[17]. M. F. Zayed, W. H. Eisa, A. M. Hezma, Spectroscopic and Antibacterial Studies of Anisotropic Gold Nanoparticles Synthesized Using Malvaparviflora, J. appl. Spectroscopy **2017**, 83, 1046 – 1050.

[18]. H. A. El-Boraey , M. A. Abdel-Hakeem , Facile synthesis, spectral, EPR, XRD and antimicrobial screening of some g-irradiated N0, N000-(1E, 2E)-1,2-diphenylethane-1,2-diylidene)bis(2-aminobenzohydrazide) metal complexes, J. Mol. Struct. 2020, 1211, 128086.

[19]. T. Manjuraj , G. Krishnamurthy, Y. D. Bodke, H. S. B. Naik , H. S. A. Kumar, Synthesis, XRD, thermal, spectroscopic studies and biological evaluation of Co(II), Ni(II) Cu(II) metal complexes derived from 2-benzimidazole, J. Mol. Stuct. **2018,** 1171, 481- 487.

[20]. O. Ozdemir, Synthesis and characterization of a new diimine Schiff base and its Cu^{2+} and Fe^{3+} complexes: Investigation of their photoluminescence,conductance,spectrophotometric and sensor behaviors,J. Mol. Struct. **2019**, 1179, 376 -389.

[21]. A. A. Alothman, E. S. Al-Farraj, W. A. Al-Onazi , Z. M. Almarhoon, A. M. Al-Mohaimeed, Spectral characterization, electrochemical, antimicrobial and cytotoxic studies on new metal (II) complexes containing N_2O_4 donor hexadentate Schiff base ligand, , Arabian Journal of Chemistry **2020**, 13, 3889 – 3902.

[22]. K. Nakamoto, Infrared and Raman Spectra of Inorganic and Coordination Compounds, 4th ed., JohnWiley, Nature. **1964,** 68, 201.

[23].] H.F. El-Shafiy, M. Shebl, Oxovanadium(IV), cerium(III), thorium(IV) and dioxouranium(VI) complexes of 1-ethyl-4-hydroxy-3-(nitroacetyl)quinolin-2(1H)-one:Synthesis, spectral, thermal, fluorescence, DFT calculations, antimicrobial and antitumor studies, J. Mol. Struct. **2018,** 1156, 403 – 417.

[24]. M. Shebl, Synthesis, spectroscopic characterization and antimicrobial activity of binuclear metal complexes of a new asymmetrical Schiff base ligand: DNA binding affinity of copper(II) complexes, Spectrochim. Acta A **2014**,117, 127.

[25]. A. W. Coats, J. P. Redfern Metal Chem. **2001**, 26, 532.

[26]. C. R. Vinodkumar, M. K. Muraleedharan Nair, P. K. Radhakrishnan, J. *Therm. Anal. Cal.***2000**, 61, 143.

[27]. A. L Sharma, I. O, singh, H. R. singh, R. M Kadam, M. K Bhide, M. D. Snstry, Transit and Sons, New York, **1986**.

[28]. S. N. Shukla, P. Gaur, M. LalRaidas, B. Chaurasia, Tailored synthesis of unsymmetrical tetradentate ONNO schiff base complexes of Fe(IIl), Co(II) and Ni(II): Spectroscopic characterization, DFT optimization, oxygen-binding study, antibacterial and anticorrosion activity, J. Mol. Struct. **2020**, 1202, 127362.

[29]. M. Shebl, Mononuclear, homo- and hetero-binuclear complexes of 1-(5-(1-(2-aminophenylimino)ethyl)-2,4-dihydroxyphenyl)ethanone: synthesis, magnetic, spectral, antimicrobial, antioxidant, and antitumor studies, *J. Coord. Chem.***2016**, 69, 199 – 214.

[30]. M. N. Ahamad , K. Iman , M. K.rRaza, M. Kumar, A. Ansari, M. Ahmad, M. Shahid, Anticancer properties, apoptosis and catecholase mimic activities of dinuclear cobalt(II) and copper(II) Schiff base complexes, Bioorg. Chem. **2020**, 95, 103561.

[31]. M. Mashaly, T. M. Ismail, S. B. E. L. Maraghy, H. A. Habib, Heteronuclear complexes of oxorhenium(V) with Fe(III), Co(II), Ni(II), Cu(II), Cd(II) and UO 2 (VI) and their biological activities. Journal of Coordination Chemistry, *J. Coord. Chem.***2004**, 57, 1099 – 1123.

[32]. R. Kalarani, M. Sankarganesh , G. G. Vinoth Kumar, M. Kalanithi, Synthesis, spectral, DFT calculation, sensor, antimicrobial and DNA binding studies of Co(II), Cu(II) and Zn(II) metal complexes with 2-amino benzimidazole Schiff base, J. Mol. Struct. **2020**, 1206, 127725.

[33]. A. B. P. Lever, Inorganic Electronic Spectroscopy, Elsevier, New York, (**1984**).

[34]. T. M. A. Ismail, Mononuclear and binuclear Co(II), Ni(II), Cu(II), Zn(II) and Cd(II) complexes of schiff-base ligands derived from 7-formyl-8-hydroxyquinoline and diaminonaphthalenes, *J. Coordination chemistry***2005**, 58,141- 151.

[35]. M. Hassanein, S. M. Abu-Wafa, corrdination chemical studies on Cu(II) complexes of some derivatives of 4-hydroxy-2(1H) quinolones, Zeitschrift fur anorganische und allgameine, chemie**1989**, 570(1), 145 – 151.

[36]. M.A. Diab, S.G. Nozha, A.Z. El-Sonbati, M.A. El-Mogazy, Sh.M. Morgan, Polymer complexes. LXXVIII. Synthesis and characterization of supramolecularuranyl polymer complexes: Determination of the bond lengths of uranyl ion in polymer complexes, ApplOrganometal Chem. 2019, e5153.

[37]. O. A. El-Gammal, G. M. Abu El-Reash, S. E. Ghazy, A. H. Radwan, Synthesis, characterization, molecular modeling and antioxidant activity of (1E,5E)-1,5-bis(1-(pyridin-2-yl)ethylidene)carbonohydrazide (H2APC) and its zinc(II), cadmium(II) and mercury(II) complexes, J. Mol. Struct. **2012**, 1020, 6–15.

[38]. T. A. Yousef, O. K. Alduaij, S. F. Ahmed, G. M. Abu El-Reash, O. A. El-Gammal, Structural, DFT and biological studies on Cr(III) complexes of semi and thiosemicarbazide ligands derived from diketohydrazide, J. Mol. Struct. 2016, 1125, 788-799.

[39]. T. H. Rakha, O. A. El-Gammal, H. M. Metwally, G. M. Abu El-Reash, Synthesis, characterization, DFT and biological studies of (Z)-N0-(2-oxoindolin-3- ylidene) picolinohydrazide and its Co(II), Ni(II) and Cu(II) complexes, J. Mol. Struct. **2014**, 1062, 96–109.

[40]. N. Raman, A. Sakthivel, K. Rajasekaran, Design , Structure elucidation DNA interactions and antimicrobial activities of metal complexes containing tetraazamacrocyclic Schiff bases, *J. Coord. Chem.***2009**, 62, 1661- 1672.

[41]. A. Kulkarni, S. A Patil, P. S. Badami,Synthesis, characterization, DNA cleavage and *in vitro* antimicrobial studies of La(III), Th(IV) and VO(IV) complexes with Schiff bases of coumarin derivatives,*Eur. J. Med. Chem.***2009**, 44, 2904-2912.

[42]. M. Hakimi, M. Alikhani , M. Mashreghi, N. Feizi, H. Raeisi, Y. Mirzai,V. Eigner, M. Dusek, A heterodinuclear complex of s-d block containing sodium(I), manganese(II) and the enrofloxacinate anion: Preparation, crystal structure and antibacterial activity, J . Mol. Struct. **2019**, 1186, 355 – 361.

[43]. S. Amer, N. El-Wakiel, H. El-Ghamry, Synthesis, Sspectral, antitumor and antimicrobial studies on Cu(II) of purine and triazole Schiff base derivatives, J. Mol. Struct. **2013**, 1049, 326 – 335.

[44]. K.M. Gilmour, Perspectives on carbonic anhydrase, comparative biochem. And physiology, A Molecular and Integrative Physiology **2010**, 157, 193 -197.

[45]. C.T. Supuran, A. Scozzafava, Carbonic anhydrases as targets for medicinal chemistry. Bioorg. Med. Chem. **2007**, 15, 4336 – 4350.

[46]. C.T. Supuran, Carbonic anhydrases: novel therapeutic applications for inhibitors and activators, Nat. Rev. Drug Discov. **2008**, 7, 168-181.

[47]. H. T. Abdel-Mohsena, A. M. El Kerdawyb, M. A. Omara, E. Berrinod, A. S. Abdelsamiea, H. I. El Diwani , C. T. Supuranm, New thiopyrimidine-benzenesulfonamide conjugates as selective carbonic anhydrase II inhibitors: synthesis, *in vitro* biological evaluation, and molecular docking studies, Bioorg. Med. Chem. **2020**, 28, 115329.

[48]. A. M. Abu-Dief, Development of Metal Oxide Nanoparticles as Semiconductors J. nanotechnol. nanomaterials, **2020**, 1(1), 5 -10.

[49]. G. Maity, P. Maji, S. Sain, S. Das, T. Kar, S. K. Pradhan, Microstructure, optical and electrical characterizations of nanocrystalline $ZnAl_2O_4$ spinel synthesized by mechanical alloying: Effect of sintering on microstructure and properties Physica E: Low-dimensional Systems and Nanostructures **2019**, 108, 411–420.